Arabian Journal of Chemistry (2021) **14**, 103105

King Saud University

Arabian Journal of Chemistry

www.ksu.edu.sa
www.sciencedirect.com

ORIGINAL ARTICLE

Green synthesis of NiO nanoparticles using *Calendula officinalis* extract: Chemical charactrization, antioxidant, cytotoxicity, and anti-esophageal carcinoma properties

Yu Zhang [a], Behnam Mahdavi [b,*], Majid Mohammadhosseini [c], Esmail Rezaei-Seresht [b], Sogand Paydarfard [b], Maryam Qorbani [b], Mohammad Karimian [d], Naser Abbasi [e], Hori Ghaneialvar [e,f], Elahe Karimi [e]

[a] *Department of Oncology, Henan Province Hospital of TCM, The Second Affiliated Hospital of Henan University of TCM, Zhengzhou City, Henan Province 450000, China*
[b] *Department of Chemistry, Faculty of Science, Hakim Sabzevari University, 96179-76487 Sabzevar, Iran*
[c] *Department of Chemistry, College of Basic Sciences, Shahrood Branch, Islamic Azad University, Shahrood, Iran*
[d] *Department of General Surgery, Faculty of Medicine, Ilam University of Medical Sciences, Ilam, Iran*
[e] *Biotechnology and Medicinal Plants Research Center, Ilam University of Medical Sciences, Ilam, Iran*
[f] *Department of Clinical Biochemistry, Faculty of Medicine, Ilam University of Medical Sciences, Ilam, Iran*

Received 11 January 2021; accepted 22 February 2021
Available online 14 March 2021

KEYWORDS

Calendula officinalis;
Esophageal cancer;
In vitro condition;
Nickel nanoparticles

Abstract In this study, nickel nanoparticles (NiONPs) have been successfully synthesized in an aqueous medium using the aqueous extract from the leaves of *Calendula officinalis*. The synthesized NiONPs were characterized using different techniques. According to the XRD analysis, the mean crystal size for NiONPs was found to be 33.17 nm. In addition, SEM images exhibited a uniform spherical morphology with a size of 60.39 nm for the NiONPs. The anti-esophageal carcinoma potentials of *C. officinalis* leaf aqueous extract, and NiONPs were assessed by the MTT assay against distal esophageal adenocarcinoma (FLO-1), gastroesophageal junction adenocarcinoma (ESO26), human caucasian esophageal carcinoma (OE33), and human esophageal squamous cell carcinoma (KYSE-270) cell lines. This study showed that NiONPs had excellent cell death and anti-cancer effects against esophageal carcinoma cell lines. The IC_{50} of NiONPs were 380, 263, 229, and 251 μg/mL against FLO-1, ESO26, OE33, and KYSE-270 cell lines, respectively. Among

* Corresponding author.
E-mail address: b.mahdavi@hsu.ac.ir (B. Mahdavi).
Peer review under responsibility of King Saud University.

Production and hosting by Elsevier

https://doi.org/10.1016/j.arabjc.2021.103105

the studied cell lines, the best anti-esophageal cancer activities of NiONPs were gained in the cell line of OE33. The antioxidant activity of NiONPs was investigated using the DPPH test. In the antioxidant test, NiONPs prevented the oxidation of 50% of the DPPH molecules at a concentration of 204 μg/mL. Considering the obtained results, it can be suggested that NiONPs may be administrated as a chemotherapeutic supplement/drug to treat esophageal carcinoma.

1. Introduction

The main esophageal diseases involve esophageal cancer, hiatus hernia, Chagas disease, Schatzki's ring, Mallory-Weiss syndrome, Nutcracker esophagus, Barrett's esophagus, Jackhammer esophagus, Boerhaave syndrome, Zenker's Diverticulum, Killian-Jamieson diverticulum as well as diffuse esophageal spasm (Zhang et al., 2012; Akhtar, 2013; Enzinger and Mayer, 2003; Pennathur et al., 2013). The severe type of esophageal cancer appears as esophageal carcinoma (Enzinger and Mayer, 2003; Pennathur et al., 2013). In this relation, familial predisposition, radiation therapy, scorching drinks, acid reflux, alcohol, obesity, smoking tobacco, and chewing betel nut are the common risk factors of esophageal carcinoma (Akhtar, 2013). The main clinical signs of esophageal carcinoma are enlarged lymph nodes around the collarbone, dry cough, vomiting blood, weight loss, hoarse voice, coughing up, and some difficulty in swallowing (Zhang et al., 2012). The positron emission tomography, magnetic resonance imaging, low-dose helical computerized tomography scan, computerized tomography, chest X-ray, esophageal endoscopic ultrasound, molecular testing, blood tests, needle biopsy, and physical and history examination are among the most commonly used techniques to diagnose esophageal carcinoma (Enzinger and Mayer, 2003; Pennathur et al., 2013).

Different procedures like surgery, targeted therapy, immunotherapy, chemotherapy, radiation etc are used in treating esophageal carcinoma and the most prescribed chemotherapeutic drugs are capecitabine, fluorouracil, carboplatin, oxaliplatin, and cisplatin (Stahl et al., 2013). However, the major drawbacks in their use are some unpleasant side effects like fatigue, hair loss, weight loss, mouth sores, diarrhea, and nausea and thereby new formulations of these drugs are of urgent necessity (Klein et al., 2014). In the search for alternative medicines, it has been found that metallic nanoparticles can exhibit excellent anticancer properties (Namvar et al., 2014). Since then, incessant investigations and reports have been undertaken to develop and synthesize metallic nanoparticles and nanocomposites to treat different cancers including esophageal carcinoma worldwide (Klein et al., 2014; Namvar et al., 2014).

Nanomaterials, which are the subject of our study, have unique competencies different from their macro-scale counterparts due to their low volume/surface ratio and many advanced as well as some physiochemical criteria such as color, solubility, strength, prevalence, toxicity, magnetic, optical, thermodynamics (El-Sayed et al., 2006; Chatterjee et al., 2012; Azizi et al., 2017). In recent years, biological methods which are basically non-toxic, cost-effective, and environmentally friendly have gained much interest compared to physicochemical nanoparticle synthesis methods (Klein et al., 2014; Namvar et al., 2014; El-Sayed et al., 2006; Chatterjee et al., 2012). Various pathways have been developed for the biogenic or biological formulation of nanomaterials from the salts of different metal ions. The synthesis of nanoparticles under purely 'green' principles can be achieved by using an environmentally compatible solvent system with environmentally-friendly stabilizing and reducing factors (Azizi et al., 2017; Sumathi et al., 2013; Roberson et al., 2014). The basic principle in the biogenesis of nanoparticles is reducing metal ions of several biomolecules found in vital organisms. In addition to reducing the environmental impact of biological synthesis, this critical step enables the production of large quantities of nanoparticles, which are well-defined in size and morphology, and independent of contamination, as well. Microorganisms, marine algae, plant extracts, plant tissue, fruits, and all plants are administrated to formulate nanomaterials (Azizi et al., 2017; Sumathi et al., 2013; Roberson et al., 2014; Chung et al., 2017). Recently, scientists have revealed that medicinal plants' green synthesized-metallic nanoparticles possess excellent anti-cancer properties. In fact, the green synthesized metallic nanoparticles have achieved notable consideration in a variety of medicinal disciplines (Chatterjee et al., 2012; Azizi et al., 2017; Sumathi et al., 2013; Roberson et al., 2014). Some relevant conducted studies have shown that some nanoparticles (Especially platin, gold, and silver nanoparticles) have promising therapeutic properties accounting for their potential use as excellent alternatives to physicochemically different metal-supported nanoparticles, antibacterial, and particularly anticancer drugs (Such as Cisplatin and Azathioprine) (Azizi et al., 2017; Sumathi et al., 2013; Roberson et al., 2014). The previous studies have indicated the anticancer effects of metallic nanoparticles against various cell lines such as Lewis lung carcinoma (LL2) cells, ADR/MCF-7 cancer cells, A549 lung epithelial cancer cell line, HT29, HCT15, HCT116, and RKO colon cancer cell lines, U87 and LN229 human glioma cancer lines, A549 cells and HeLa cells, HepG2-R, HDF together with C0045C, 4 T1 mouse mammary carcinoma and A549, H460, and H520 human lung cancer cells (Sumathi et al., 2013; Roberson et al., 2014; Chung et al., 2017). A brief survey of the literature demonstrates that no study has been performed on the remedial capacities of natural compounds green-synthesized nickel nanoparticles in treating esophageal cancers so far. The study of Chen et al. (Chen et al., 2013) revealed the anti-immortalized myelogenous leukemia activities of nickel nanoparticles green-synthesized by *Tsoong* herb against K562 cell line in the *in vitro* condition. In addition, the previous nickel nanoparticles treated the leukemic mice for less than 20 days (Chen et al., 2013). In the study of Rameshthangam and Pandian Chitra (Rameshthangam and Pandian Chitra, 2018), the leaf extract of medicinally important plant *Ocimum*

sanctum (O. sanctum) has been used to synthesis the nickel nanoparticles and extraction of quercetin. quercetin has been conjugated with nickel nanoparticles for enhanced anticancer effect on human breast cancer MCF–7 cells. Extracted quercetin was conjugated with polyethylene glycol coated nickel nanoparticles (quercetin–polyethylene glycol–nickel nanoparticles) used as carriers for breast cancer treatment. Anticancer activity of quercetin–polyethylene glycol–nickel nanoparticles was evaluated by assessing cell viability, reactive oxygen species (ROS) production, caspase activity, mitochondrial membrane potential (MMP) and changes in nuclear morphology (staining methods). 0.85 mg of quercetin was extracted from 1 g of leaves with a retention time (R_t) of 2.914 min. Loading and encapsulation efficiency of quercetin onto polyethylene glycol–nickel nanoparticles was 15.04% and 82% respectively and quercetin–polyethylene glycol–nickel nanoparticles have shown a sustained release of quercetin of about 84% after 48 h. quercetin and quercetin–polyethylene glycol–nickel nanoparticles showed dose-dependent (1.56–50 μg/mL) anticancer effect against MCF–7 cells with IC_{50} values of 50 and 6.25 μg/mL respectively which was mediated by oxidative stress due to ROS over-production that induced loss of mitochondrial membrane potential, caspase −9, −7 activities leading to apoptosis (Rameshthangam and Pandian Chitra, 2018). In another study, a co-treatment of sodium nitroprusside and 5-fluorouracil resulted in inhibition of the cytotoxic effect of 5-fluorouracil, while a combination treatment of nickel nanoparticles with Na_2S, sodium nitroprusside, and 5-fluorouracil caused highly significant cytotoxicity against colorectal cancer cell lines. Direct sequencing reveals new mutations, mainly intronic variation in endothelial NO synthase gene that has not previously been described in the database. These findings indicate that H_2S promotes the anticancer efficiency of 5-fluorouracil in the presence of nickel nanoparticles while NO has antiapoptotic activity in colorectal cancer cell lines (Housein et al., 2021).

Calendula officinalis is a short-lived aromatic herbaceous perennial, growing to 80 cm (31 in) tall, with sparsely branched lax or erect stems. The leaves are oblong-lanceolate, 5–17 cm (2–7 in) long, hairy on both sides, and with margins entire or occasionally waved or weakly toothed. The inflorescences are yellow, comprising a thick capitulum or flowerhead 4–7 cm diameter surrounded by two rows of hairy bracts; in the wild plant they have a single ring of ray florets surrounding the central disc florets (Al-Snafi, 2015). *Calendula officinalis* is widely cultivated and can be grown easily in sunny locations in most kinds of soils. Although perennial, it is commonly treated as an annual, particularly in colder regions where its winter survival is poor, and in hot summer locations where it also does not survive. In traditional medicines, some people use the leaf of *Calendula officinalis* for the prevention, control, and cure of various cancers such as breast, ovarian, prostate, and blood cancers (Al-Snafi, 2015). The main antioxidant and anticancer compounds of *C. officinalis* are aromadendrene, bisabolol oxide bornyl acetate, butanone, α-cadinol, T-cadinol, calacorene, alamenene, camphene, camphor, *trans*-caryophyllene, 1,8-cineole, α-copaene, cubebene,β-cubebene, cubenol, *epi*-cubenol, *p*-cymene, eudesmol, β-farnesene, β-fenchene, α-humulene, α-gurjunene, limonene, menthone, α-muurolene, α-muurolol, T-muurolol, myrcene, nerolidol,*cis*-β-ocimene, *trans*-β-ocimene,α-patchoulene, pentan-2-one, α-pinene, β-pinene, α-phellandrene, β-phellandrene, sabinene,α-terpinene, γ-terpinene, terpinene-4-ol, terpinolene, and β-ylangene (Al-Snafi, 2015).

The present experiment was conducted to evaluate the possible anti-esophageal carcinoma activity of synthesized nickel nanoparticles using an aqueous extract prepared from the leaves of *C. Officinalis* against common cell lines of esophageal carcinoma including FLO-1, ESO26, OE33, and KYSE-270.

2. Materials and methods

2.1. Material

Bovine serum, 2,2-diphenyl-1-picrylhydrazyl (DPPH), dimethyl sulfoxide (DMSO), decamplmaneh fetal, 4-(dimethylamino) benzaldehyde, hydrolyzate, antimycotic antibiotic solution, Ehrlich solution, and borax-sulfuric acid mixture, DMED, all were afforded from the US Sigma-Aldrich company.

2.2. Preparation and extraction of the aqueous extract of *C. Officinalis leaf*

To obtain the aqueous extract of the plant, 250 g portions of the dried branches of the *C. officinalis* leaves were poured into a container containing 2000 mL boiled water, and the container lid was tightly closed for 4 h. Then, the content of the container was filtered, and the remaining liquid was placed on a bain-marie to evaporate. Finally, a tar-like material was obtained, which was powdered by a freeze dryer.

2.3. Preparation and optimization of *NiONPs synthesis*

The green synthesis of nickel nanoparticles was carried out according to a previous study with some modifications (Ezhilarasi et al., 2016). The synthesis was optimized at different operations factors, including extract concentrations and time. Accordingly, 3 mL of the extract (0.05–0.15 g/mL) was added to 10 mL of $NiSO_4{\cdot}6H_2O$ (15 mM) using deionized water. In the next step, one mL of NaOH (2%) was added dropwise and stirred for 10 min. The reaction mixture was placed in an ultrasonic bath (75 W) for 5–20 min and the synthesized green nickel oxide nanoparticles were subsequently precipitated. The obtained NiONPs were washed three times with water and centrifuged at 10000 rpm for 15 min. Finally, the obtained precipitate was dried at 75 °C.

2.4. Chemical characterization techniques

UV–Vis. and FT-IR spectroscopy; XRD, SEM, and EDS techniques were used to characterize the biosynthesized NiONPs. Different parameters of the nanoparticles, such as shape, particle size, fractal dimensions, crystallinity and surface area were evaluated by these techniques. The FT-IR spectra were recorded using a Shimadzu FT-IR 8400 over the range of 400–4000 cm^{-1}(KBr disc), while MIRA3TESCAN-XMU was used to report the FE-SEM images and EDS-based assessments. The XRD pattern of NIONPs was recorded in the 2θ range of 20-80° using a GNR EXPLORER instrument at a voltage of 40 kV, a current of 30 mA, and Cu-Kαradiation (1.5406 Å).

2.5. Measurement of cell toxicity of NiONPs

In the present study, the anti-human esophageal carcinoma and cytotoxicity potentials of $NiSO_4{\cdot}6H_2O$, *C. officinalis* leaf aqueous extract, and NiONPs were assessed by the MTT assay against normal (HUVEC) and esophageal carcinoma (human esophageal squamous cell carcinoma (KYSE-270), distal esophageal adenocarcinoma (FLO-1), gastroesophageal junction adenocarcinoma (ESO26), and human caucasian esophageal carcinoma (OE33)) cell lines under *in vitro* condition. They were then cultured as a monolayer culture in 90% RPMI-1640 medium and 10% fetal serum and were immediately after supplemented with 200 mg/mL streptomycin, 125 mg/mL penicillin, and 8 mg/mL amphotericin B. The culture was then exposed to 0.5 atmospheric carbon dioxide at 37 °C, on which the tests were performed after at least ten successful passages. MTT was an assay used to investigate the toxic effects of various materials on various cell lines, including non-cancer and cancer cells. To evaluate the cell toxicity effects of the compounds used in this research, the cells were transferred from the T25 flask to the 96-well flasks. In each cell of the 96-cell flasks, 7000 cells of cancer and fibroblast cell lines were cultured, and the volume of each cell was eventually increased to 100 µL. Before treating the cells in the 96-well flak, the density of cells was increased to 70%, so the 96-well flasks were incubated for 24 h to obtain the cell density of 7×10^3. Thereafter, the initial culture medium was discarded, and variable concentrations (0–1000 µg/mL) of $NiSO_4{\cdot}6H_2O$, *C. officinalis* leaf aqueous extract, and NiONPs were incubated at 37 °C and 5% CO_2 for 24, 48, and 72 h. Then, 20 µL MTT was added to each well. This step was followed by the addition of 100 µL of DMSO solvent to each well. The treated wells were then kept at room temperature for 25 min and read at 490 and 630 nm by a microtitre plate reader. The cell lines were also treated with the hydroalcoholic extract (1.25 mg/mL), which inhibited about 20% of the cell growth. Annexin/PI method was used to determine the apoptosis level in the treated and control cell lines using a flow cytometry machine. Under the optimized experimental conditions, the cell lines were treated with variable concentrations (0–1000 µg/mL) of $NiSO_4{\cdot}6H_2O$, *C. officinalis* leaf aqueous extract, and NiONPs for 24 h. Cells were irrigated with phosphate-buffered saline (PBS). After centrifugation, buffer binding was added to the obtained precipitate. Then, 5 µL Annexin V dye was added and incubated for 15 min at 25 °C. Cells were washed with the binding solution, following with the addition of 10 µL of PI dye. Finally, cell analysis was conducted by a flow cytometry machine according to the below formula (Arulmozhi et al., 2013):

$$\text{Cellviability } (\%) = \frac{\text{SampleA.}}{\text{ControlA.}} \times 100 \quad (1)$$

2.6. Investigation of the antioxidant capacity of NiONPs

The DPPH method is a common method for assessing the antioxidant activity of plant species and metallic nanoparticles. It is based on trapping the free radical of 2,2-diphenyl-1-picrylhydrazyl (DPPH), using antioxidant agents which reduce the absorption rate at a wavelength of 520 nm. When the DPPH solution is mixed with a material that can donate hydrogen atom, radical resuscitation is formed, followed by color reduction. This reaction eliminates the purple color whose index is forming an absorption band at 520 nm (Hosseinimehr et al., 2011). To determine the radical scavenging activity of the $NiSO_4{\cdot}6H_2O$, *C. officinalis* leaf aqueous extract, and NiONPs, 1 mL of 50 µm DPPH was combined with 1 mL of variable concentrations (0–1000 µg/mL) of $NiSO_4{\cdot}6H_2O$, *C. officinalis* leaf aqueous extract and NiONPs. Then, they were transferred to the 37 °C for 1 h. The samples absorption rate was determined at 520 nm by a spectrophotometer, and the antioxidant activity was calculated using the following formula (Hosseinimehr et al., 2011):

$$\text{Inhibition } (\%) = \frac{\text{SampleA.}}{\text{ControlA.}} \times 100 \quad (2)$$

The blank sample contained 1 mL methanol and 1 mL $NiSO_4{\cdot}6H_2O$, *C. officinalis* leaf aqueous extract, and NiONPs, and a sample of 1 mL DPPH and 2 mL $NiSO_4{\cdot}6H_2O$, *C. officinalis* leaf aqueous extract, and NiONPs with the applied concentrations were regarded as the negative control.

Calculation of half-maximal inhibitory concentration (IC_{50}) is a suitable method for comprising the activity of pharmaceutical-based materials. In this method, the measurement and comparison criterion is the concentration in which 50% of the final activity of the drug occurs. In this experiment, the IC_{50} of various repeats is estimated and compared with the IC_{50} of BHT, which is introduced as the antioxidant activity index. The closer is the obtained value to the IC_{50} of BHT, the stronger is the antioxidant activity of the material. The graph of the IC_{50} of the extract was produced by drawing the percent inhibition curve versus the extract concentration. First, three stock samples with variable concentrations (0–1000 µg/mL) of $NiSO_4{\cdot}6H_2O$, *C. officinalis* leaf aqueous extract, and NiONPs were prepared. Then, a serial dilution was prepared from each sample, and IC_{50} of the above samples was measured separately, and finally their mean was calculated. BHT, with different concentrations, was considered positive control. All experiments were performed in triplicate.

2.7. Statistical analysis

The obtained results were analyzed by SPSS (version 20) software using one-way ANOVA, followed by Duncan posthoc test ($P \leq 0.01$).

3. Results and discussion

3.1. Optimization of NiONPs synthesis

To evaluate the conditions for NiONPs synthesis, we first examined the

reaction among 3 mL of the extract (0.05 g/mL), 10 mL $NiSO_4{\cdot}6H_2O$ (15 mM), and 1 mL NaOH (2%). The reaction was optimized at different operations factors, including *C. officinalis* extract concentration and reaction time. The results are presented in Table 1. According to the results, the best result (82 mg) was achieved using *C. officinalis* extract in the concentration of 0.1 g/ mL after 15 min.

Table 1 The optimization of the reaction conditions for the synthesis of NiONPs.

Entry	Extract Con. g/ mL	Time Min.	Yield mg
1	0.05	5	31
2	0.1	5	50
3	0.15	5	52
4	0.1	10	64
5	0.15	10	66
6	0.1	15	82
7	0.15	15	82
8	0.1	20	82
9	0.15	20	82

3.2. Characterization of NiONPs

3.2.1. UV–visible spectroscopy analysis

The UV–Vis. spectra of biosynthesized NiNPs using the aqueous extract of *C. officinalis* are shown in Fig. 1. The surface plasmon resonance of NiONPs was confirmed by UV–Vis. and compared with a previous report, the appearance of a band at the wavelength of 357 nm approved forming NiONPs (Sharmila et al., 2019).

FT-IR Analysis. In FT-IR spectra of metal oxides, the vibration band for metal–oxygen bond usually appears in 400 to 700 cm-1. Fig. 2 presents the spectra of NiONPs. The peaks at 445, 538, and 648 cm-1 are attributed to the bending vibration of Ni-O. These peaks for iron oxide nanoparticles have been reported previously with a small difference in the respective wavenumber (Nwanya et al., 2020; Juibari and Eslami, 2019; Sabouri et al., 2019). FT-IR spectroscopy is a reliable strategy to evaluate the plant secondary metabolites as the capping and reducing agents of nickel sulfate precursor to NiONPs. According to the findings of this report, the FT-IR spectra of NiONPs and *C. officinalis* extract were very similar to each other confirming the successful biosynthesis of the nickel oxide nanoparticles. The presence of different-IR bands correlates with the existence of various functional groups in *C. officinalis* extract. For instance, peaks at 3417 and 2925 cm^{-1}

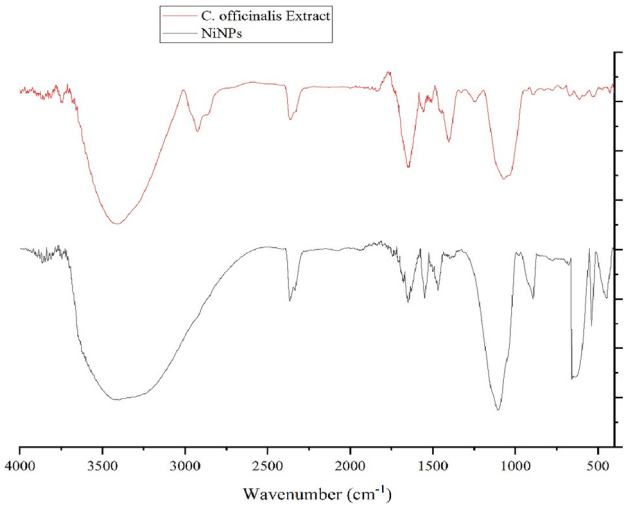

Fig. 2 FT-IR Spectrum of NiONPs and C. officinalis extract.

are related to O-H and aliphatic C-H stretching; peaks at a range of 1471 to 1662 cm-1 correspond to C = C and C = O stretching, while a peak at 1096 cm^{-1} could be ascribed to -C-O stretching. These peaks can be generally considered to confirm the presence of various valuable natural compounds such as phenolic, flavonoid, saponins, quinones, terpenoids which have been reported previously in a number of plant extracts (de Oliveira Carvalho et al., 2018; Długosz et al., 2018; Verma et al., 2018). In the biosynthesis process of metallic nanoparticles, the secondary metabolite of plant extracts, as reducing, stabilizing and dispersing agents usually bind to NPs through their functional groups of hydroxyl and carbonyl (Ghidan et al., 2016).

3.2.2. XRD analysis

Fig. 3 shows the XRD pattern of the biosynthesized NiONPs which approve the synthesis of nickel oxide. The peaks at 2θ values of 27.12, 37.42, 43.68, 63.02 and 75.45 are indexed as (1 1 0), (1 1 1), (2 0 0), (2 2 0), and (3 1 1) planes and are matched as well as to those of standard database JCPDS card no. 1313–991. The crystallinity of the NiONPs has been accepted using

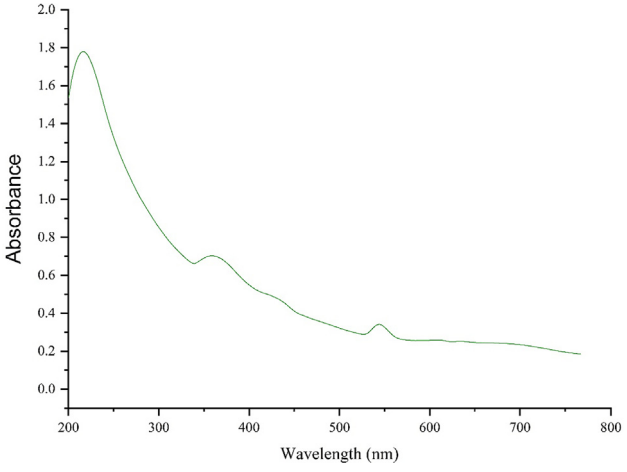

Fig. 1 UV–Vis. spectra of biosynthesized NiONPs.

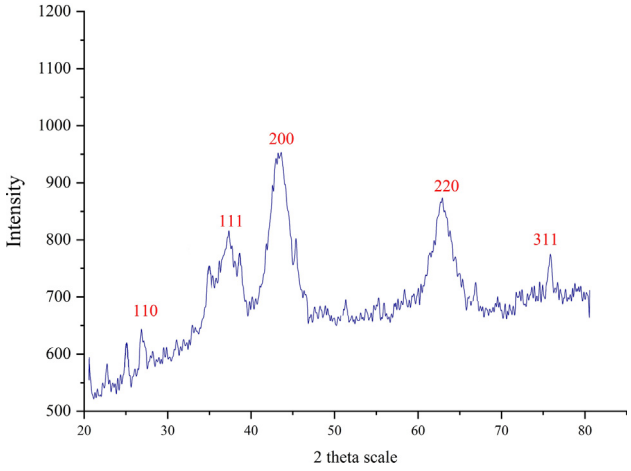

Fig. 3 XRD pattern of the biosynthesized NiONPs.

the XRD diffractogram. The peaks at different degrees have also been previously reported (Nwanya et al., 2020; Iqbal et al., 2019; Baranwal et al., 2018). The average crystal size of NiNPs was calculated using X-Ray diffraction according to the Scherrer equation.

$$D = \frac{k\lambda}{\beta cos\theta} \quad (3)$$

Where k, λ, βand θ account for the Scherrer's constant (k = 0.9), the wavelength of X-ray radiation (λ = 0.15406 n m), the full-width at half-maximum of the corresponding plane (in radians), the characteristic X-ray radiation, respectively. The NiONPs had an average crystal size 33.17 nm. In our literature review, researchers have reported various crystal size for the biosynthetic NiONPs according to the relevant XRD patterns. In turn, the mean crystal size of 16.9–43.9 nm has been reported for the synthetically synthesized NiONPs using okra plant extract (Sharmila et al., 2019), 10–56 nm for *Ocimum sanctum* (Rameshthangam and Chitra, 2018), 18–20 nm for *Terminalia Chebula* (Ibraheem et al., 2019), 24 nm for *Rhamnus virgate* (Iqbal et al., 2019), 18.26 nm for dry silk extract (Nwanya et al., 2020), and 24 nm for 8–8.3 nm for guar gum (Baranwal et al., 2018).

3.2.3. SEM analysis

TEM and FE-SEM images of NiONPs shown in Fig. 4 (a ,b) depict a spherical morphology for the prepared NiONPs reported previously (Rameshthangam and Chitra, 2018). The figure also confirms the uniformity, well-dispersed, and homogeneity of the NiONPs. Like the other metallic nanoparticles being synthesized using green chemistry approaches, a tendency to aggregate is observed for NiONPs. This property has been reported for other types of biosynthesized nanoparticles, *viz*. NiONPs, ZnNPs, AgNPs, MnNPs, and SnNPs (Iqbal et al., 2019; Mahdavi et al., 2020; Mahdavi et al., 2019; Baghayeri et al., 2018; Ahmeda et al., 2020).

On average, the diameter of particle size for NiONPs was 60.39 nm.In our review of literature, different sizes have been reported for the biosynthesized NiONPs, e.g., 18.6 nm for synthetic NiONPs using okra plant extract (Sabouri et al., 2019), 48–72 nm for *Ocimum sanctum* (Rameshthangam and Chitra, 2018), 20–25 nm for *Terminalia Chebula* (Ibraheem et al., 2019), and 24 nm for *Rhamnus virgate* (Iqbal et al., 2019).

The EDS analysis is usually known as a semi-quantitative technique to recognize the elements of the synthesized nanoparticles. Using EDS (see Fig. 5), the elemental composition profile of the biosynthetic NiONPs showed the presence of nickel biosynthesized NPs considering the signals appearing at 0.8, 7.5, and 8.2 keV and corresponding to the Lα, Kα, and Kβ peaks of nickel.

These signals are in agreement with a previous study on synthesized NiONPs using dry silk extract (Nwanya et al., 2020).Furthermore, a single at 0.52 Kev belongs to oxygen which can be attributed to the oxygen in iron oxide nanoparticles and to the organic molecules present in *C. officinalis* extract that linked to the surface of NiONPs. The presence of carbon on the surface of NiONPs was also approved by the signal at 0.28 Kev.

3.3. Antioxidant properties of NiONPs against DPPH

In the present study, the DPPH free-radical scavenging potential of *C. officinalis* leaf aqueous extract and NiONPs in a wide range of concentrations revealed impressive prevention similar to that of BHT as a standard antioxidant agent. Free-radicals are molecules that do not have a complete electron shell and are capable of increasing the chemical reaction compared to others. They are formed if the human body is exposed to tobacco smoke and radiation. In humans, the most important free radical is oxygen. When an oxygen molecule (O_2) is exposed to radiation, it removes an electron from the other molecules, destroying DNA and other molecules. Some of these changes may cause a number of persistent diseases, e.g. heart problems, muscle failure, diabetes and cancer (Hosseinimehr et al., 2011). Antioxidants act like a broom against free radicals and have been recognized as powerful remedies to destroy free radicals and regenerate the damaged cells. More importantly, laboratory evidence has shown that antioxidants can highly prevent cancer (Chung et al., 2017;

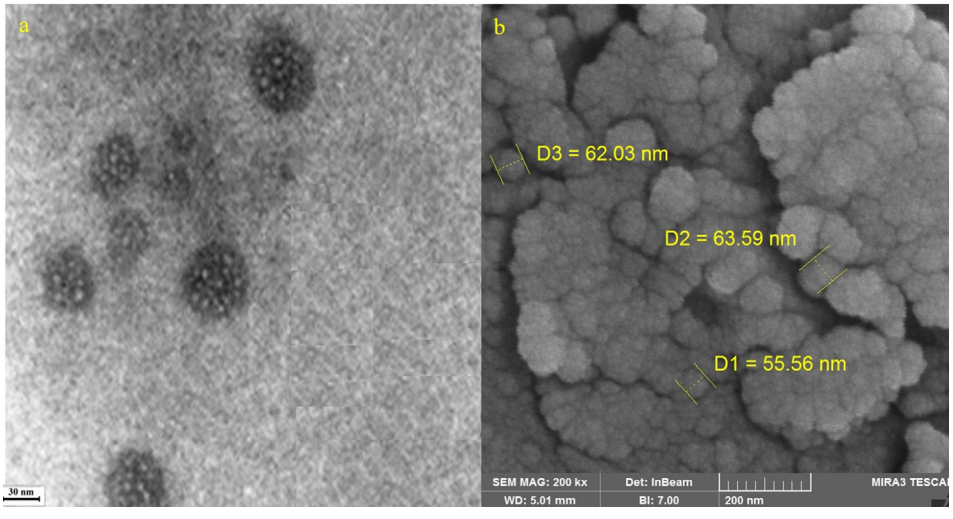

Fig. 4 a: TEM Image of NiONPs; b: FE-SEM Image of NiONPs.

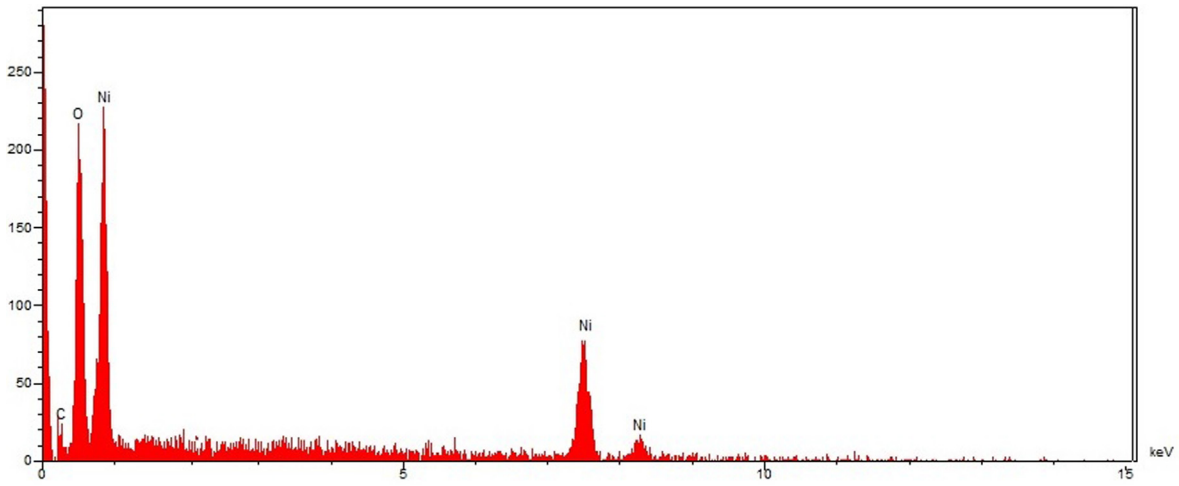

Fig. 5 EDS analysis of NiONPs.

Chen et al., 2013; Rameshthangam and Pandian Chitra, 2018; Housein et al., 2021).The IC_{50} of *C. officinalis* leaf aqueous extract, BHT, and NiONPs were 328, 204, and 192 μg/mL, respectively (Fig. 6; Table 2).

Metallic nanoparticles also have excellent potential to inhibit DPPH. The results obtained in our study are in line with many studies in which the mutual effect has been monitored to increase the antioxidant capacities between herbs and metallic salts against DPPH (Chung et al., 2017; Chen et al., 2013; Rameshthangam and Pandian Chitra, 2018; Housein et al., 2021).

In general, metallic nanoparticles display remarkable and extraordinary antioxidant impacts, among which the antioxidant effects of NiONPs have been well-documented. When NiONPs are synthesized with medicinal plants, the nickel element forms a very strong bond with flavonoid and phenolic compounds, creating unique antioxidant effects. In a previous study, it was indicated that *C. officinalis* is a rich source of antioxidant compounds including terpenoids compounds which were formerly mentioned. It is also noteworthy that the excellent antioxidant properties of *C. officinalis* leaf aqueous extract can be attributed to the presence of these valuable natural compounds (Al-Snafi, 2015). Several studies were carried out in the nanotechnology field using various medicinal plants, but to the best of our knowledge, no report is available on NiONPs synthesized using *C. officinalis* leaf aqueous extract.

3.4. Cytotoxicity potential of NiONPs nanoparticles

In our study, the treated cells with several concentrations of the present nickel salt, *C. officinalis*, and NiONPs were examined by MTT test for 48 h regarding the cytotoxicity properties on normal (HUVEC) and esophageal carcinoma (human esophageal squamous cell carcinoma (KYSE-270), distal esophageal adenocarcinoma (FLO-1), gastroesophageal junction adenocarcinoma (ESO26), and human caucasian esophageal carcinoma (OE33) cell lines (Tables 3 and 4). The absorbance was read at 570 nm, which indicated extraordinary viability on normal cell line (HUVEC) even up to 1000 μg/mL for nickel salt, *C. officinalis*, and NiONPs.

In colon cancer cell lines, their viability decreased dose-dependently in the presence of nickel salt, *C. officinalis*, and NiONPs. The IC_{50} of *C. officinalis* and NiONPs against the KYSE-270 cell line were 521 and 251 μg/mL whereas 831 and 380 μg/mL for human FLO-1cell line, respectively. Additionally, the numerical IC_{50} values of *C. officinalis* and NiONPs were found to be 763 and 264 μg/mL vs. ESO26 cell line and 584 and 229 μg/mL vs. OE33 cell line, respectively. A simple perusal of the obtained results demonstrates that the best $IC_{50}$of cytotoxicity property of NiONPs was seen in the case of the OE33 cell line against the above-used cell lines.

Most probably the significant anti-colon cancer potentials of NiONPs synthesized by *C. officinalis* aqueous extract against esophageal cancer cell lines are linked to their antioxidant activities. Similar studies have revealed the antioxidant materials such as metallic nanoparticles especially NiONPs and ethnomedicinal plants reduce the volume of tumors by removing free radicals (Katata-Seru et al., 2018). The high presence of free radicals in the normal cells makes many mutations in their DNA and RNA, destroying their gene expression, and then accelerating the proliferation and growth of abnormal or cancerous cells.

The prevalence of free radicals in different types of cancer such as skin, throat, ovarian, testicular, bladder, colon, small intestine, gastrointestinal stromal, stomach, breast, lung, vaginal, prostate, pancreatic, liver, gallbladder, hypopharyngeal, fallopian tube, thyroid, esophageal, parathyroid, bile duct, and rectal cancers indicates the significant role of these molecules in making angiogenesis and tumorigenesis (Sangami and Manu, 2017; Beheshtkhoo et al., 2018).

Many researchers reported NiONPs synthesized by ethnomedicinal plants with high antioxidant compounds have a remarkable role in removing free radicals and growth inhibition of all cancerous cells (Sangami and Manu, 2017; Beheshtkhoo et al., 2018; Radini et al., 2018).

Among the various agents of metallic nanoparticles such as, surface functions nature, texture, size, and morphology, the size efficacy is of prime significance in the anticancer tests. In this context, the previous reports have shown that the anticancer property enhances with a reduction in size of particle-based on their better penetration property through the cell

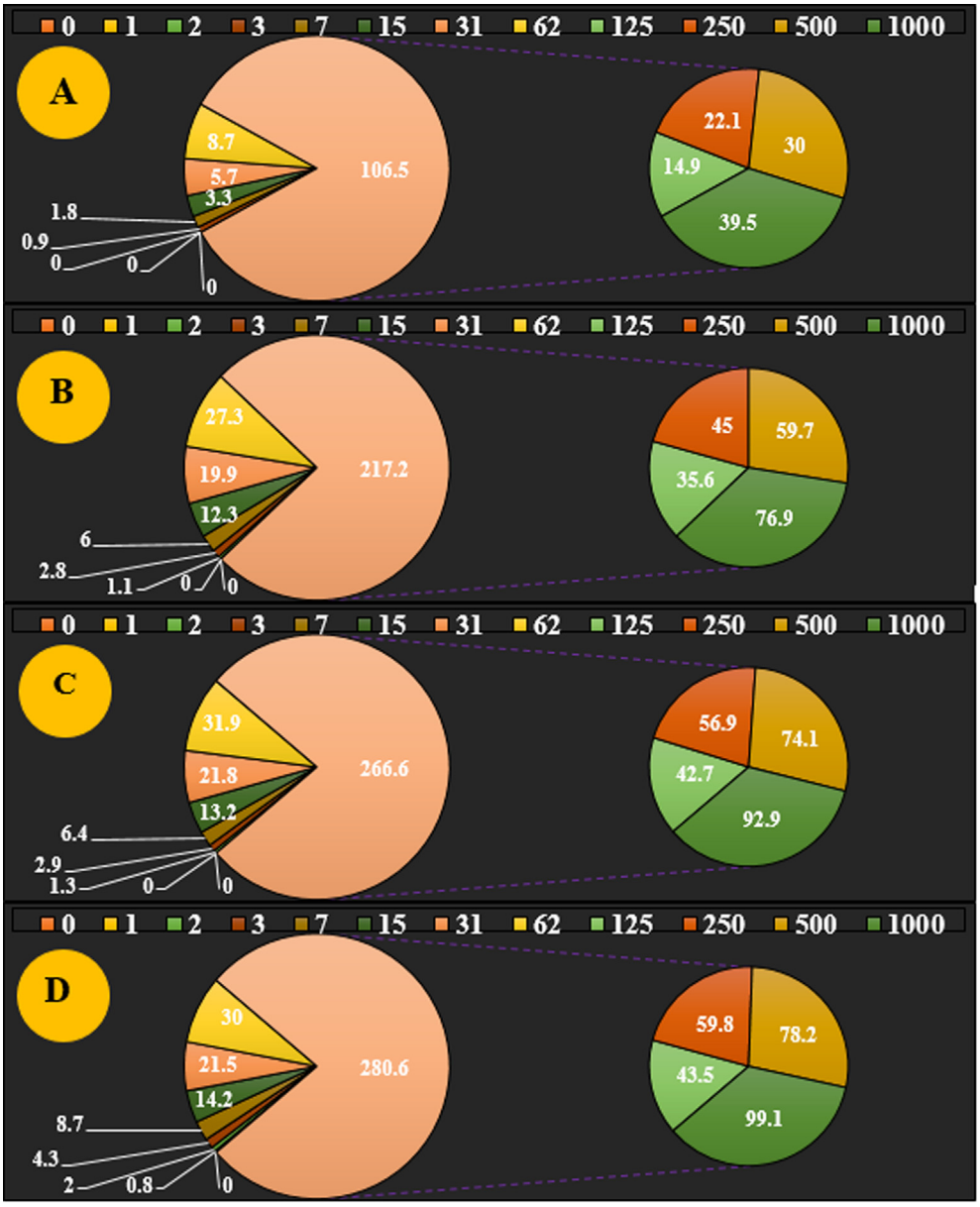

Fig. 6 The antioxidant properties of $NiSO_4$ (A), *C. officinalis* leaf aqueous extract (B), NiONPs (C), and BHT (D) against DPPH.

Table 2 The IC_{50} of $NiSO_4$, *C. officinalis* leaf aqueous extract, NiONPs, and BHT in the antioxidant test.

	$NiSO_4$ μg/mL	*C. officinalis* μg/mL	NiONPs μg/mL	BHT μg/mL
IC_{50} against DPPH	–	328 ± 0[a]	192 ± 0[b]	204 ± 0[b]

lines. Moreover, it has been determined that the size of particle lower than 100 nm demonstrates a better effect in the corresponding cancer cell lines (Sangami and Manu, 2017; Beheshtkhoo et al., 2018; Radini et al., 2018). As shown in Figs. 4 and 5 of the present study, the sizes of nickel biosynthesized nanoparticles by *C. officinalis* leaf aqueous extract is at the average size of 60.39 nm.

4. Conclusions

In this research, the nickel nanoparticles were attained from the reaction of *C. officinalis* leaf extract (1 g in 10 mL of water) and $NiSO_4$(15 mM)·$6H_2O$. To evaluate the main characteristics of the synthesized nanoparticles, FE-SEM, UV–Vis, and FT-IR methods were utilized and the relevant results revealed

Table 3 The anti-esophageal carcinoma properties of $NiSO_4$, *C. officinalis* leaf aqueous extract, and NiONPs against the human esophageal carcinoma cell line.

Concentration μg/ml	Cell Viability (%)				
	HUVEC	FLO-1	ESO26	OE33	KYSE-270
$NiSO_4$(0)	100 ± 0^{a}	100 ± 0^{a}	100 ± 0^{a}	100 ± 0^{a}	100 ± 0^{a}
$NiSO_4$(1)	100 ± 0^{a}	100 ± 0^{a}	100 ± 0^{a}	100 ± 0^{a}	100 ± 0^{a}
$NiSO_4$(2)	99.2 ± 0.44^{a}	100 ± 0^{a}	100 ± 0^{a}	100 ± 0^{a}	100 ± 0^{a}
$NiSO_4$(3)	98.6 ± 0.89^{a}	99.4 ± 0.54^{a}	100 ± 0^{a}	99.2 ± 0.83^{a}	100 ± 0^{a}
$NiSO_4$(7)	95 ± 1.22^{a}	98.6 ± 1.14^{a}	99 ± 0.7^{a}	98.2 ± 0.83^{a}	99.4 ± 0.54^{a}
$NiSO_4$(15)	92.2 ± 0.83^{a}	96 ± 1^{a}	97.6 ± 0.89^{a}	95.6 ± 0.89^{a}	97.2 ± 0.44^{a}
$NiSO_4$(31)	88.2 ± 1.3^{a}	93.2 ± 0.83^{a}	94.2 ± 1.3^{a}	91.6 ± 0.89^{a}	93 ± 1.22^{a}
$NiSO_4$(62)	83.2 ± 0.44^{a}	90 ± 1.22^{a}	90.6 ± 0.89^{a}	86.2 ± 0.44^{a}	87.2 ± 0.44^{a}
$NiSO_4$(125)	77.8 ± 1.09^{ab}	85 ± 0.7^{a}	84.4 ± 0.89^{a}	80.2 ± 1.3^{ab}	80.4 ± 0.89^{ab}
$NiSO_4$(250)	71.4 ± 0.89^{ab}	80.8 ± 1.09^{ab}	78 ± 0.7^{ab}	74.8 ± 1.09^{ab}	73.4 ± 0.89^{ab}
$NiSO_4$(500)	64.6 ± 0.89^{ab}	74.4 ± 0.89^{ab}	70.2 ± 0.83^{ab}	66 ± 1^{ab}	66.2 ± 1.3^{ab}
$NiSO_4$(1000)	53.4 ± 0.54^{b}	66.6 ± 1.14^{ab}	61.8 ± 1.09^{ab}	56.6 ± 0.89^{b}	55.4 ± 0.54^{b}
C. officinalis(0)	100 ± 0^{a}	100 ± 0^{a}	100 ± 0^{a}	100 ± 0^{a}	100 ± 0^{a}
C. officinalis(1)	100 ± 0^{a}	100 ± 0^{a}	100 ± 0^{a}	100 ± 0^{a}	100 ± 0^{a}
C. officinalis(2)	100 ± 0^{a}	100 ± 0^{a}	100 ± 0^{a}	100 ± 0^{a}	100 ± 0^{a}
C. officinalis(3)	99.2 ± 0.83^{a}	99.2 ± 1.3^{a}	99 ± 1.22^{a}	99.4 ± 0.89^{a}	98.2 ± 0.44^{a}
C. officinalis(7)	99.8 ± 1.09^{a}	98.8 ± 1.09^{a}	98 ± 1^{a}	98.6 ± 1.14^{a}	96 ± 1^{a}
C. officinalis(15)	98.2 ± 1.3^{a}	96.2 ± 0.44^{a}	96.2 ± 0.83^{a}	95.8 ± 1.09^{a}	92.2 ± 0.44^{a}
C. officinalis(31)	98.6 ± 0.89^{a}	93.4 ± 0.54^{a}	92.6 ± 0.89^{a}	90.2 ± 0.44^{a}	87.2 ± 0.44^{a}
C. officinalis(62)	97 ± 1^{a}	88 ± 0.7^{a}	87.2 ± 1.3^{a}	85.6 ± 0.89^{a}	81 ± 1^{a}
C. officinalis(125)	96.2 ± 0.44^{a}	80.6 ± 0.89^{ab}	79.2 ± 0.44^{ab}	78.2 ± 0.44^{ab}	72.8 ± 1.09^{ab}
C. officinalis(250)	95.6 ± 1.14^{a}	71 ± 1^{ab}	69 ± 1.22^{ab}	67.4 ± 0.89^{ab}	62.2 ± 0.44^{ab}
C. officinalis(500)	93.6 ± 1.14^{a}	60.2 ± 0.83^{b}	57.8 ± 1.09^{b}	53.2 ± 0.44^{b}	51.2 ± 1.3^{b}
C. officinalis(1000)	91.4 ± 0.89^{a}	45.2 ± 0.44^{b}	40.2 ± 0.44^{bc}	36.6 ± 1.14^{bc}	37 ± 0.7^{bc}
NiONPs (0)	100 ± 0^{a}	100 ± 0^{a}	100 ± 0^{a}	100 ± 0^{a}	100 ± 0^{a}
NiONPs (1)	100 ± 0^{a}	100 ± 0^{a}	100 ± 0^{a}	100 ± 0^{a}	100 ± 0^{a}
NiONPs (2)	100 ± 0^{a}	99.2 ± 0.83^{a}	99.2 ± 0.83^{a}	99.6 ± 1.14^{a}	99.4 ± 0.54^{a}
NiONPs (3)	100 ± 0^{a}	97.4 ± 0.89^{a}	97.6 ± 0.89^{a}	98.8 ± 1.09^{a}	97.2 ± 0.44^{a}
NiONPs (7)	99.2 ± 1.3^{a}	94.6 ± 1.14^{a}	94.2 ± 0.44^{a}	95 ± 1.22^{a}	94.2 ± 1.3^{a}
NiONPs (15)	98.4 ± 0.54^{a}	89.2 ± 0.44^{a}	88.8 ± 1.09^{a}	90.2 ± 0.83^{a}	89.4 ± 0.89^{a}
NiONPs (31)	98.4 ± 0.89^{a}	82.4 ± 0.89^{a}	80 ± 1^{ab}	81 ± 1^{a}	81.6 ± 0.89^{a}
NiONPs (62)	97.2 ± 0.44^{a}	74.8 ± 1.09^{ab}	71 ± 0.7^{ab}	71.6 ± 0.89^{ab}	70.2 ± 0.44^{ab}
NiONPs (125)	95.8 ± 1.09^{a}	66 ± 1.22^{ab}	61.6 ± 1.14^{ab}	59.4 ± 0.54^{b}	60.8 ± 1.09^{b}
NiONPs (250)	92.6 ± 0.89^{a}	56 ± 0.7^{b}	51.8 ± 1.09^{b}	47.4 ± 0.89^{b}	50.2 ± 1.3^{b}
NiONPs (500)	88.6 ± 1.14^{a}	44.2 ± 1.3^{b}	38 ± 1^{bc}	32.6 ± 0.89^{bc}	35.6 ± 1.14^{bc}
NiONPs (1000)	83 ± 1.22^{a}	28.2 ± 0.44^{bc}	22.6 ± 0.89^{c}	14.8 ± 1.09^{c}	18 ± 0.7^{c}

that nickel nanoparticles had been successfully synthesized. Base on the FT-IR spectrum the presence of a great number of antioxidant compounds produced appropriate conditions for reducing nickel. In the FE-SEM technique, the mean size of nickel nanoparticles was assessed to be 60.39 nm, which is favorable. On the other hand, the nickel nanoparticles showed the best antioxidant activities against DPPH. Nickel nanoparticles had appropriate anti-esophageal carcinoma activities dose-dependently against esophageal carcinoma (human esophageal squamous cell carcinoma (KYSE-270), distal esophageal adenocarcinoma (FLO-1), gastroesophageal junction adenocarcinoma (ESO26), and human caucasian esophageal carcinoma (OE33)) cell lines without any cytotoxicity on the normal cell line (HUVEC). Regarding the findings of our study, nickel nanoparticles containing *C. officinalis* leaf aqueous extract may be utilized as an efficient drug/supplement in treating colon cancer and diseases in humans after sufficient clinical studies.

Table 4 The IC_{50} of $NiSO_4$, *C. officinalis* leaf aqueous extract, and NiONPs in cytotoxicity and anti-esophageal carcinoma tests.

	$NiSO_4$ μg/mL	***C. officinalis* μg/mL**	**NiONPs μg/mL**
IC_{50} against HUVEC	–	–	–
IC_{50} against FLO-1	–	831 ± 0^{a}	380 ± 0^{d}
IC_{50} against ESO26	–	736 ± 0^{b}	264 ± 0^{e}
IC_{50} against OE33	–	584 ± 0^{c}	229 ± 0^{e}
IC_{50} against KYSE-270	–	521 ± 0^{c}	251 ± 0^{e}

Declaration of Competing Interest

The authors declare that they have no known competing financial interests or personal relationships that could have appeared to influence the work reported in this paper.

References

Zhang, H.-Z., Jin, G.-F., Shen, H.-B., 2012. Epidemiologic differences in esophageal cancer between Asian and Western populations. Chinese journal of cancer 31, 281.

Akhtar, S., 2013. Areca nut chewing and esophageal squamous-cell carcinoma risk in Asians: A meta-analysis of case–control studies. Cancer Causes Control 24, 257–265.

Enzinger, P.C., Mayer, R.J., 2003. Esophageal cancer. N. Engl. J. Med. 349, 2241–2252.

Pennathur, A., Gibson, M.K., Jobe, B.A., Luketich, J.D., 2013. Oesophageal carcinoma. The Lancet 381, 400–412.

Stahl, M., Mariette, C., Haustermans, K., Cervantes, A., Arnold, D., 2013. Oesophageal cancer: ESMO Clinical Practice Guidelines for diagnosis, treatment and follow-up†. Ann. Oncol. 24, 51–56.

Klein, S., Sommer, A., Distel, L.V., Hazemann, J.-L., Kröner, W., Neuhuber, W., Müller, P., Proux, O., Kryschi, C., 2014. Superparamagnetic iron oxide nanoparticles as novel X-ray enhancer for low-dose radiation therapy. J. Phys. Chem. B 118, 6159–6166.

Namvar, F., Rahman, H.S., Mohamad, R., Baharara, J., Mahdavi, M., Amini, E., Chartrand, M.S., Yeap, S.K., 2014. Cytotoxic effect of magnetic iron oxide nanoparticles synthesized via seaweed aqueous extract. Int. J. Nanomed. 9, 2479.

El-Sayed, I.H., Huang, X., El-Sayed, M.A., 2006. Selective laser photo-thermal therapy of epithelial carcinoma using anti-EGFR antibody conjugated gold nanoparticles. Cancer Lett. 239, 129–135.

Chatterjee, A.K., Sarkar, R.K., Chattopadhyay, A.P., Aich, P., Chakraborty, R., Basu, T., 2012. A simple robust method for synthesis of metallic copper nanoparticles of high antibacterial potency against E. coli. Nanotechnology 23, 085103.

Azizi, M., Ghourchian, H., Yazdian, F., Dashtestani, F., AlizadehZeinabad, H., 2017. Cytotoxic effect of albumin coated copper nanoparticle on human breast cancer cells of MDA-MB 231. PLoS ONE 12, e0188639.

Sumathi, S., Dharani, B., Sivaprabha, J., Raj, K.S., Padma, P., 2013. Cell death induced by methanolic extract of Prosopis cineraria leaves in MCF-7 breast cancer cell line. Int J Pharmacol Sci Invent 2, 21–26.

Roberson, M., Rangari, V., Jeelani, S., Samuel, T., Yates, C., 2014. Synthesis and characterization silver, zinc oxide and hybrid silver/zinc oxide nanoparticles for antimicrobial applications. Nano Life 4, 1440003.

Chung, I.M., Abdul Rahuman, A., Marimuthu, S., Vishnu Kirthi, A., Anbarasan, K., Padmini, P., Rajakumar, G., 2017. Green synthesis of copper nanoparticles using Eclipta prostrata leaves extract and their antioxidant and cytotoxic activities. Experimental and therapeutic medicine 14, 18–24.

Chen, M., Zhang, Y., Huang, B., Yang, X., Wu, Y., Liu, B., Yuan, Y., Zhang, G., 2013. Evaluation of the antitumor activity by Ni nanoparticles with verbascoside. Journal of Nanomaterials 2013.

Rameshthangam, P., Pandian Chitra, J., 2018. Synergistic anticancer effect of green synthesized nickel nanoparticles and quercetin extracted from Ocimum sanctum leaf extract. J Mater Sci Technol. 34, 508–522.

Housein, Z., Kareem, T.S., Salihi, A., 2021. In vitro anticancer activity of hydrogen sulfide and nitric oxide alongside nickel nanoparticle and novel mutations in their genes in CRC patients. Sci Rep 11, 2536.

Al-Snafi, A., 2015. The chemical constituents and pharmacological effects of Calendula officinalis-A review. Indian Journal of Pharmaceutical Science & Research 5, 172–185.

Ezhilarasi, A.A., Vijaya, J.J., Kaviyarasu, K., Maaza, M., Ayeshamariam, A., Kennedy, L.J., 2016. Green synthesis of NiO nanoparticles using Moringa oleifera extract and their biomedical applications: Cytotoxicity effect of nanoparticles against HT-29 cancer cells. J. Photochem. Photobiol., B 164, 352–360.

Arulmozhi, V., Pandian, K., Mirunalini, S., 2013. Ellagic acid encapsulated chitosan nanoparticles for drug delivery system in human oral cancer cell line. KB. Colloids Surf., B 110, 313–320.

Hosseinimehr, S.J., Mahmoudzadeh, A., Ahmadi, A., Ashrafi, S.A., Shafaghati, N., Hedayati, N., 2011. The radioprotective effect of Zataria multiflora against genotoxicity induced by γ irradiation in human blood lymphocytes. Cancer Biother. Radiopharm. 26, 325–329.

Sharmila, G., Thirumarimurugan, M., Muthukumaran, C., 2019. Green synthesis of ZnO nanoparticles using Tecoma castanifolia leaf extract: characterization and evaluation of its antioxidant, bactericidal and anticancer activities. Microchem. J. 145, 578–587.

Nwanya, A.C., Ndipingwi, M.M., Ikpo, C.O., Obodo, R., Nwanya, S. C., Botha, S., Ezema, F.I., Iwuoha, E.I., Maaza, M., 2020. Zea mays lea silk extract mediated synthesis of nickel oxide nanoparticles as positive electrode material for asymmetric supercabattery. J. Alloy. Compd. 822, 153581.

Juibari, N.M., Eslami, A., 2019. Synthesis of nickel oxide nanorods by Aloe vera leaf extract. J. Therm. Anal. Calorim. 136, 913–923.

Sabouri, Z., Akbari, A., Hosseini, H.A., Hashemzadeh, A., Darroudi, M., 2019. Eco-friendly biosynthesis of nickel oxide nanoparticles mediated by okra plant extract and investigation of their photocatalytic, magnetic, cytotoxicity, and antibacterial properties. J. Cluster Sci. 30, 1425–1434.

de Oliveira Carvalho, H., Góes, L.D.M., Cunha, N.M.B., Ferreira, A. M., Fernandes, C.P., Favacho, H.A.S., Junior, J.O.C.S., Ortiz, B. L.S., Navarrete, A., Carvalho, J.C.T., 2018. Development and standardization of capsules and tablets containing Calendula officinalis L. hydroethanolic extract. Revista Latinoamericana de Química 46, 16–27.

Długosz, M., Markowski, M., Pączkowski, C., 2018. Source of nitrogen as a factor limiting saponin production by hairy root and suspension cultures of Calendula officinalis L. Acta Physiologiae Plantarum 40, 35.

Verma, P.K., Raina, R., Agarwal, S., Kaur, H., 2018. Phytochemical ingredients and Pharmacological potential of Calendula officinalis Linn. Pharmaceutical and Biomedical Research 4, 1–17.

Ghidan, A.Y., Al-Antary, T.M., Awwad, A.M., 2016. Green synthesis of copper oxide nanoparticles using Punica granatum peels extract: Effect on green peach Aphid. Environ. Nanotechnol. Monit. Manage. 6, 95–98.

Iqbal, J., Abbasi, B.A., Mahmood, T., Hameed, S., Munir, A., Kanwal, S., 2019. Green synthesis and characterizations of Nickel oxide nanoparticles using leaf extract of Rhamnus virgata and their potential biological applications. Appl. Organomet. Chem. 33, e4950.

Baranwal, K., Dwivedi, L.M., Singh, V., 2018. Guar gum mediated synthesis of NiO nanoparticles: An efficient catalyst for reduction of nitroarenes with sodium borohydride. Int. J. Biol. Macromol. 120, 2431–2441.

Rameshthangam, P., Chitra, J.P., 2018. Synergistic anticancer effect of green synthesized nickel nanoparticles and quercetin extracted from Ocimum sanctum leaf extract. J. Mater. Sci. Technol. 34, 508–522.

Ibraheem, F., Aziz, M.H., Fatima, M., Shaheen, F., Ali, S.M., Huang, Q., 2019. In vitro Cytotoxicity, MMP and ROS activity of green synthesized nickel oxide nanoparticles using extract of Terminalia chebula against MCF-7 cells. Mater. Lett. 234, 129–133.

Mahdavi, B., Paydarfard, S., Zangeneh, M.M., Goorani, S., Seydi, N., Zangeneh, A., 2020. Assessment of antioxidant, cytotoxicity, antibacterial, antifungal, and cutaneous wound healing activities of green synthesized manganese nanoparticles using Ziziphora clinopodioides Lam leaves under in vitro and in vivo condition. Appl. Organomet. Chem. 34, e5248.

Mahdavi, B., Saneei, S., Qorbani, M., Zhaleh, M., Zangeneh, A., Zangeneh, M.M., Pirabbasi, E., Abbasi, N., Ghaneialvar, H., 2019. Ziziphora clinopodioides Lam leaves aqueous extract mediated synthesis of zinc nanoparticles and their antibacterial, antifungal, cytotoxicity, antioxidant, and cutaneous wound healing properties under in vitro and in vivo conditions. Appl. Organomet. Chem. 33, e5164.

Baghayeri, M., Mahdavi, B., Hosseinpor-Mohsen Abadi, Z., Farhadi, S., 2018. Green synthesis of silver nanoparticles using water extract of Salvia leriifolia: Antibacterial studies and applications as catalysts in the electrochemical detection of nitrite. Appl. Organomet. Chem. 32, e4057.

Ahmeda, A., Mahdavi, B., Zaker, F., Kaviani, S., Hosseini, S., Zangeneh, M.M., Zangeneh, A., Paydarfar, S., Moradi, R., 2020. Chemical characterization and anti-hemolytic anemia potentials of tin nanoparticles synthesized by a green approach for bioremediation applications. Appl. Organomet. Chem. 34, e5433.

Katata-Seru, L., Moremedi, T., Aremu, O.S., Bahadur, I., 2018. Green synthesis of iron nanoparticles using Moringa oleifera extracts and their applications: removal of nitrate from water and antibacterial activity against Escherichia coli. J. Mol. Liq. 256, 296–304.

Sangami, S., Manu, B., 2017. Synthesis of Green Iron Nanoparticles using Laterite and their application as a Fenton-like catalyst for the degradation of herbicide Ametryn in water. Environ. Technol. Innovation 8, 150–163.

Beheshtkhoo, N., Kouhbanani, M.A.J., Savardashtaki, A., Amani, A. M., Taghizadeh, S., 2018. Green synthesis of iron oxide nanoparticles by aqueous leaf extract of Daphne mezereum as a novel dye removing material. Appl. Phys. A 124, 363.

Radini, I.A., Hasan, N., Malik, M.A., Khan, Z., 2018. Biosynthesis of iron nanoparticles using Trigonella foenum-graecum seed extract for photocatalytic methyl orange dye degradation and antibacterial applications. J. Photochem. Photobiol., B 183, 154–163.